Article

Journal of
Nanoscience and Nanotechnology
Vol. 17, 1668–1673, 2017
www.aspbs.com/jnn

Influence of Al and Mg Addition on Thermoelectric Properties of Higher Manganese Silicides Obtained by Reactive Sintering

S. Battiston[1], S. Boldrini[1,*], M. Saleemi[2,3], A. Famengo[1], S. Fiameni[1], M. S. Toprak[2], and M. Fabrizio[1]

[1] National Research Council of Italy—Institute of Condensed Matter Chemistry and Technologies for Energy, Corso Stati Uniti 4, 35127 Padova, Italy
[2] Department of Materials and Nano Physics, KTH Royal Institute of Technology, Kista-Stockholm, Sweden
[3] Department of Materials and Environmental Chemistry, Stockholm University, Stockholm, Sweden

Higher manganese silicides (HMS), represented by $MnSi_x$ ($x = 1.71$–1.75), are promising *p*-type candidates for thermoelectric (TE) energy harvesting systems at intermediate temperature range. The materials are very attractive as they may replace lead based compounds due to their non-toxicity, low cost of starting materials, and high thermal and chemical stability. Dense pellets were obtained through fast reactive sintering by spark plasma sintering (SPS). The addition –or nano-inclusion, of Al and Mg permitted the figure of merit enhancement of the material obtained with this technique, reaching the highest value of 0.40 at 600 °C. Morphology, composition and crystal structure of the samples were characterized by electron microscopies, energy dispersive X-ray spectroscopy, and X-ray diffraction analyses, respectively.

Keywords: Manganese Silicide, Thermoelectricity, SPS, Reactive Sintering.

1. INTRODUCTION

Thermoelectric generators (TEGs) are solid-state devices with no moving parts, they are noiseless, reliable and scalable, and they are good candidates for small-sized application for distributed power generation.[1] Silicide-based alloys are promising candidates for TE energy conversion at the intermediate temperature range (300–600 °C). In particular, they are very attractive as they could replace lead-based compounds due to their non-toxicity, as well as low cost of starting materials. Higher manganese silicides (HMS), represented by $MnSi_x$ ($x = 1.71$–1.75) with a chimney-ladder structure, are promising *p*-type leg candidates for intermediate temperature TE devices due to their large Seebeck coefficient, low resistivity and high oxidation resistance.[2–4]

Our previous paper[5] showed how one-step synthesis and sintering (reactive sintering), performed by a short lasting Spark Plasma Sintering (SPS) process, could be a valuable way to obtain HMS pellets with good TE performance, avoiding long lasting thermal treatments.[6,7] In this work, a low energy ball milling was carried out in order to induce a mechanical activation of the precursor powders, avoiding completely the mechanical alloying which can be detrimental for the final resulting material.[8] The morphological and TE properties of the obtained dense polycrystalline pellets were evaluated as a function of the SPS holding time, since the influence of other parameters were already previously discussed.[5] Furthermore, HMS pellets with the addition of Al and Mg are presented and discussed in this work. The role of Al-addition was already reported in several works,[9–12] indicating that it could replace Si atoms increasing the charge carrier concentration, thus leading to electrical conductivity enhancement. Al seems to play this role up to a maximum solubility limit of roughly 0.15 wt%.[9] For concentrations higher than 0.15 wt%, Al segregates at the grain boundaries in the form of aluminum oxide, increasing the phonon scattering phenomena and leading to a figure of merit ($ZT = \alpha^2\rho^{-1}\kappa^{-1}T$, where α is the Seebeck coefficient, ρ the electrical resistivity and κ the thermal conductivity) enhancement, reaching the maximum reported value of 0.7 at 500 °C.[11] The purpose of this work is to obtain Al- and Mg-doped HMS thermoelectric materials with enhanced TE performances employing reactive sintering by SPS, and exploiting the oxidation phenomena which can easily occur for more reactive elements during the process, as shown previously.[13]

*Author to whom correspondence should be addressed.

 1533-4880/2017/17/1668/006 doi:10.1166/jnn.2017.13730

2. EXPERIMENTAL DETAILS

2.1. Synthesis

HMS pellets were produced starting from Si powder (99.999%, 325 mesh, Alfa Aesar) and Mn powder (99.95%, 325 mesh, Alfa Aesar). The powders were milled with Si:Mn molar ratio of 1.73 under Ar atmosphere in a planetary ball mill (BM) with hexane as dispersion medium (WC jar, 330 rpm for 8 h). Afterwards, reactive sintering process was carried out via Spark Plasma Sintering (SPS, Dr Sinter 2050) at 900 °C and 90 MPa in a graphite die (heating rate of 100 °C min^{-1} and free cooling process) for 0, 5, 10 and 20 minutes of holding time. 10 minutes of holding time was chosen to prepare Al- and Mg-added samples in order to obtain compaction density higher than 90% and to be sure that the dopant elements could diffuse and homogenously dope the HMS matrix. In particular, Al and Mg powders were added to Mn and Si powder before the milling process following the stoichiometry: $Mn(Al_xSi_{1-x})_{1.73}$, where x was equal to 0.005, 0.010 and 0.002 which corresponded to 0.23 wt%, 0.45 wt%, and 0.90 wt%, respectively. Analogously, for the $Mn(Mg_xSi_{1-x})_{1.73}$, x was equal to 0.010 and 0.020, which correspond to 0.41 wt%, and 0.81 wt%, respectively.

2.2. Characterization

The crystalline phases were revealed by X-ray diffraction (XRD) using a Philips PW 3710 X-Ray diffractometer with Bragg-Brentano geometry and a Cu Kα source (40 kV, 30 mA). The Rietveld refinement on the XRD profiles has been exploited to obtain information of amount of various phases, crystallite sizes and theoretical densities of samples.[14] The pellet densities were estimated through the geometrical method.

The morphological and compositional characterizations were performed by Sigma Zeiss field emission scanning electron microscope (FE-SEM) equipped with Oxford X-Max energy dispersive spectroscopy (EDS) system. Focused ion beam scanning electron microscopy (FIB-SEM) was utilized to prepare a sample for transmission electron microscopy (TEM) analysis. 5 μm long and 2 μm thick layer of sample was cut from the polished surface of 1% Al-HMS sample. Platinum (Pt) metal was used to weld the cut sample with the TEM specimen grid. High resolution transmission electron microscopy (HRTEM) analysis was carried out by Jeol 2100 with an accelerating voltage of 200 keV, mapping and elemental composition analysis was performed with coupled EDS detector.

The thermal diffusivity a of the samples was measured by a laser flash thermal diffusivity system (Netzsch LFA 457 MicroFlash®). The thermal conductivity κ was calculated according to the formula $\kappa = adC_p$ where d is the density and C_p the specific heat of the material. The specific heat was calculated by means of the Netzsch Proteus Analysis software, comparing the samples with the standard material Netzsch Pyroceram 9606. The declared relative uncertainty of diffusivity measures was 3%, 5% for specific heat.

The Seebeck coefficient, α, and the electrical resistivity, ρ, were simultaneously measured from RT to 600 °C with a relative uncertainty of 5% and 10% respectively, using a custom test apparatus described elsewhere.[15] All measurements were carried out under Ar atmosphere. The combined uncertainty for ZT was 15% finally.

3. RESULTS AND DISCUSSION

The low energy ball milling process (330 rpm for 8 h) decreased the precursor particle size from tens of microns to few microns (Fig. 1) and the XRD

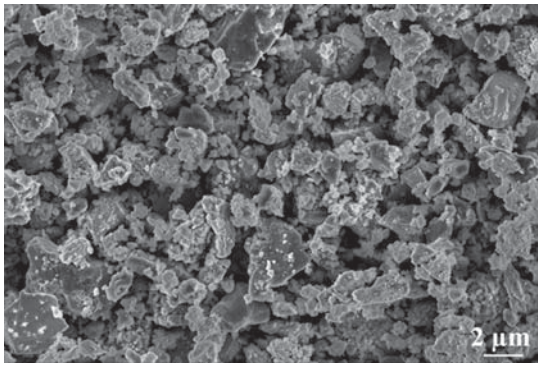

Figure 1. Secondary electron micrograph of Mn and Si powders after ball milling.

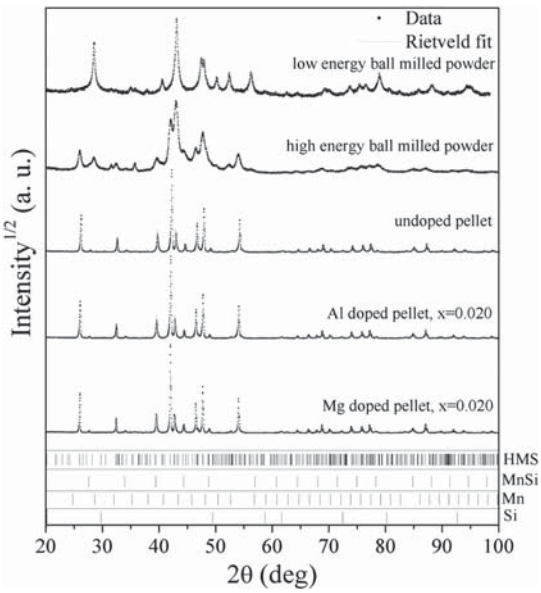

Figure 2. XRD patterns of precursor powders after ball milling at low energy (330 rpm for 8 h), and at high energy (400 rpm for 18 h). XRD patterns of undoped and doped HMS pellets, obtained with a SPS holding time of 10 min, are also presented.

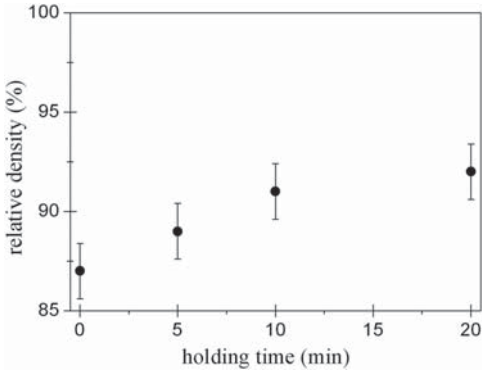

Figure 3. Relative density of undoped samples as a function of SPS holding time at 900 °C and 90 MPa.

characterization (Fig. 2) confirmed that no solid-state reaction occurred, except for a small quantity of MnO formation (below 1 wt%), as previously observed.[5]

Figure 2 also presents the XRD pattern of the precursor powders after high energy ball milling (400 rpm for 18 h). Increasing the energy of the milling process led to a mechanical alloying that was detrimental for the TE properties of the final material, since it increased the amount of MnSi phase,[16] as observed also by other authors.[8] Indeed, the higher energy milled powders showed a MnSi content of 7 wt% (the Mn, Si, and HMS phase amounts were 34 wt%, 8 wt% and 51 wt%, respectively) and the respective pellet (described and discussed elsewhere[4, 5, 16, 17]) showed 10 wt% of the MnSi metallic phase.

The pellet relative densities increased with SPS holding time, exceeding 90% after 10 min (Fig. 3). On the other hand, the grain size did not change dramatically, remaining in the range of few microns (Fig. 4).

The phase amount evaluation, performed by Rietveld refinement, showed that all sintered samples have 95 wt% of HMS TE tetragonal phase and 5 wt% of metallic cubic

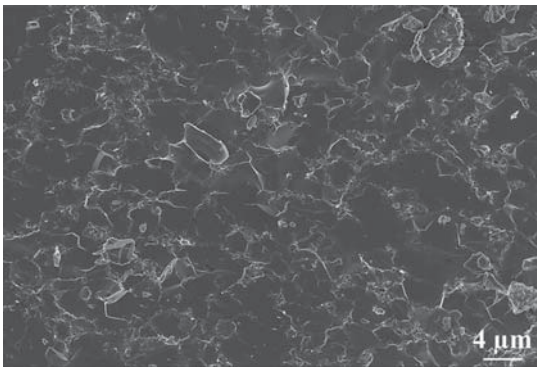

Figure 4. Secondary electron micrograph of fractured undoped sample obtained at 10 min holding time.

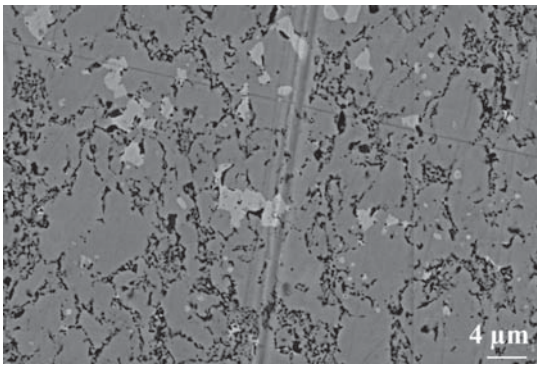

Figure 5. Backscattered electron micrograph of polished undoped sample obtained at 10 min holding time; the brighter phase is MnSi, as identified by EDS quantitative analyses.

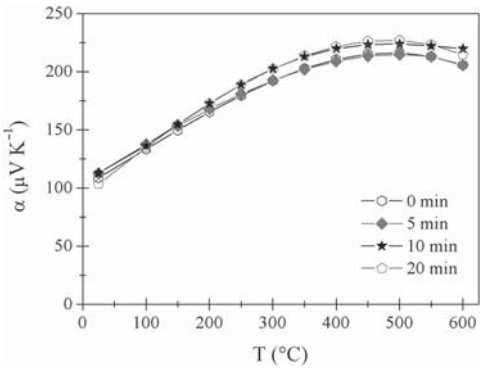

Figure 6. Seebeck coefficient as a function of temperature for undoped sintered pellets.

MnSi phase. The two phases are clearly observable in the electron micrograph of the polished sample (Fig. 5).

The XRD analyses (Fig. 2) of the Al- and Mg-added samples did not reveal the presence of these elements or their compounds. Indeed, the patterns did not show any significant difference compared to undoped samples, probably because of the low content of elements and to their

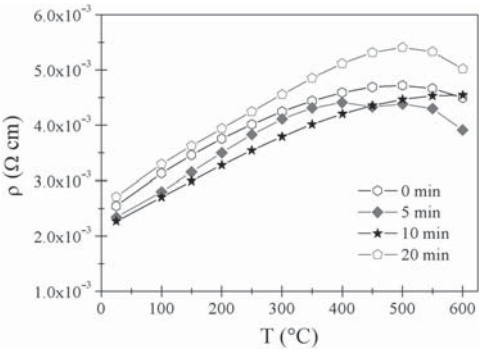

Figure 7. Electrical resistivity as a function of temperature for undoped sintered pellets.

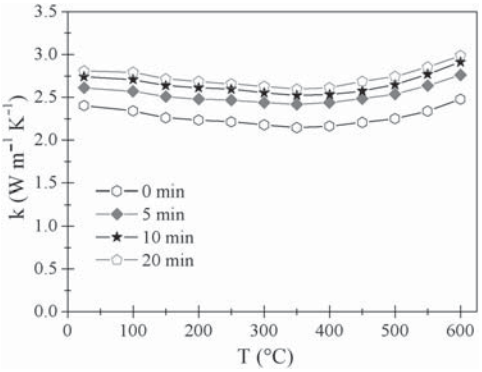

Figure 8. Thermal conductivity as a function of temperature for undoped sintered pellets.

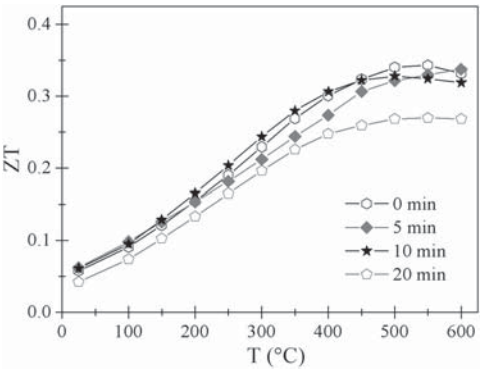

Figure 9. Figure of merit, ZT, as a function of temperature for the undoped sintered pellets.

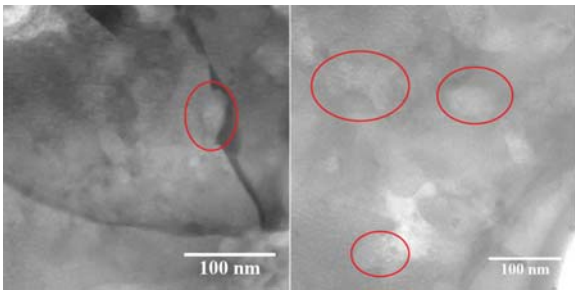

Figure 11. TEM images of sample $Mn(Al_xSi_{1-x})_{1.73}$ with $x = 0.010$ where some aluminum oxide clusters are encircled for clarity.

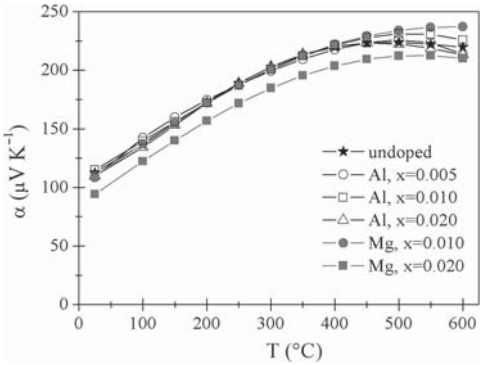

Figure 12. Seebeck coefficient as a function of temperature for doped sintered pellets.

dimensions being similar to Si. Thus, 10 min as holding time seemed a reasonably long time to allow the Al and Mg atom introduction in the HMS lattice with a resulting pellet relative density over 90%.

The measured Seebeck coefficients, α, (Figs. 6 and 12), were in agreement with the typical *p*-type conduction mechanism of this material.[4,5,16] The electrical resistivity, ρ, (Figs. 7 and 13), increased up to 500 °C with a degenerate semiconductor behavior.[18] Above 500 °C the intrinsic conduction became effective and consequently the electrical resistivity decreased. The C_p values of the LFA measured samples showed a standard deviation lower than the declared Netzsch uncertainty (5%). For this reason, the average C_p values as a function of temperature were employed for each sample. Thermal conductivity values of the undoped samples (Fig. 8) seemed not affected by holding time, with the exception of 0 min sample, which displayed lower k probably due to its lower density. Similarly, holding time seemed to not affect the ZT

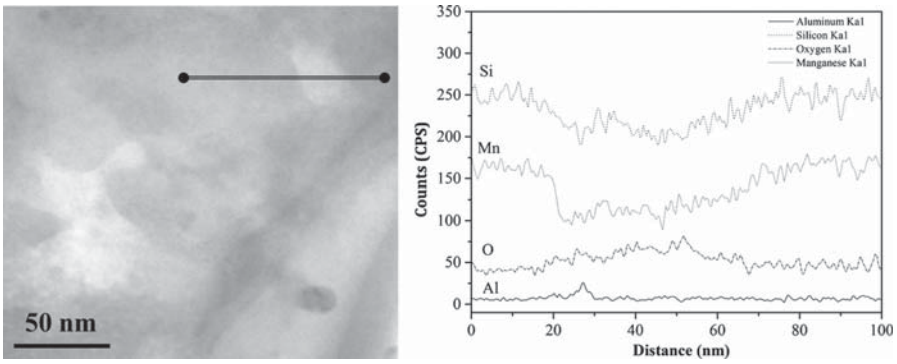

Figure 10. EDS-TEM line scan of sample Al-added with $x = 0.010$ where an aluminum oxide cluster is clearly observable.

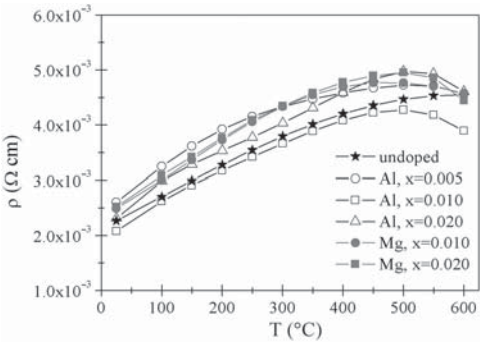

Figure 13. Electrical resistivity as a function of temperature for doped sintered pellets.

of undoped materials (Fig. 9), with the exception of the 20 min sample, which showed slightly higher resistivity at higher temperatures.

The Al- and Mg-addition did not show a clear and univocal effect on material properties, probably because those elements can be present both as lattice substituents (dopants) and as inhomogeneously dispersed oxide clusters of several tens of nanometers, as observed by EDS-TEM analyses (Figs. 10 and 11), resulting in competitive effects on the TE properties of the material. The XRD analyses could not reveal the signals of such oxides because of their low diffraction intensity, related to their low quantity, overwhelmed by the preponderant HMS XRD pattern. If compared to other samples, the Mg- added pellet with $x = 0.020$ showed lower α values and Al-added pellet, with $x = 0.010$, lower ρ values over 500 °C. Nevertheless, the sample values of α, ρ and k (Figs. 12–14 respectively) were quite similar to each other.

The resulting figure of merits, ZT, of all sintered pellets (Figs. 10 and 15) showed small dispersion of the values. The introduction of Al and Mg seemed to be ineffective in increasing the ZT of the material overall, with the exception of the Al- and Mg-addition with $x = 0.010$, which slightly improved the ZT at 600 °C from 0.32 up to 0.40

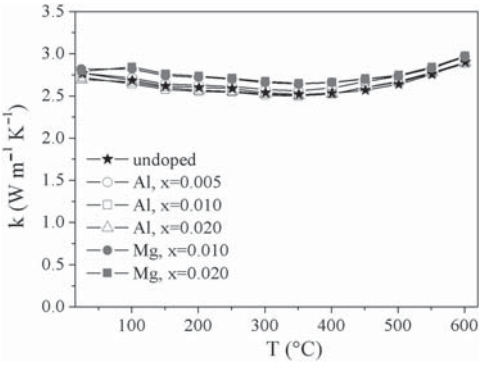

Figure 14. Thermal conductivity as a function of temperature for doped sintered pellets.

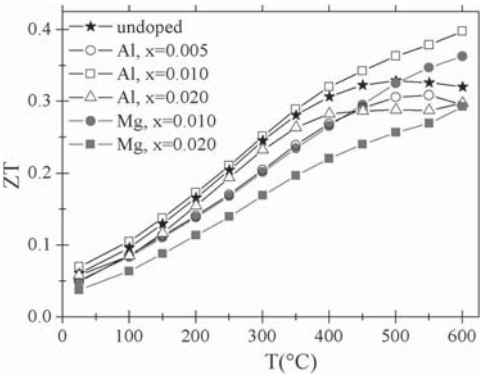

Figure 15. Figure of merit, ZT, as a function of temperature for the doped sintered pellets.

and 0.36, respectively. This behavior could probably be due to the favorable balances between the doping and the presence of oxides.

4. CONCLUSIONS

Both undoped and doped polycrystalline HMS pellets were prepared employing commercial Mn and Si powders directly by reactive sintering performed by a short lasting SPS process, avoiding long lasting thermal treatments. The maximum ZT value attained was 0.40 at 600 °C for the Al added sample with $x = 0.01$ (similar result was obtained by Shin et al.[12]) whilst Mg-added one with $x = 0.01$ reached 0.36, probably due to the favorable balances between the doping of the material and the presence of inhomogeneously dispersed oxide cluster. Nevertheless, it was confirmed that the HMS reactive sintering by SPS technique is a very promising method to obtain thermoelectric material with good ZT values, avoiding further time consuming processes.

Acknowledgments: The authors are grateful to Dr. Agresti for the inestimable help for the Rietveld refinements and professor Johnsson (Stockholm University) for his valuable discussion on SPS parameters. This work has been funded by the Italian National Research Council—Italian Ministry of Economic Development Agreement "Ricerca di sistema elettrico nazionale" and Swedish Foundation for Strategic Research—SSF for Scalable TEG project (EM11-0002) and Swedish Energy Agency for Mg_2Si project (project nr: 36656-1).

References and Notes

1. G. J. Snyder and E. S. Toberer, *Nat. Mater.* 7, 105 **(2008)**.
2. L. D. Ivanova, *Inorg. Mater.* 47, 965 **(2011)**.
3. A. Zhou, T. Zhu, X. Zhao, and E. Mueller, *J. Mater. Res.* 26, 1900 **(2011)**.
4. Z. Zamanipour, X. Shi, M. Mozafari, J. S. Krasinski, L. Tayebi, and D. Vashaee, *Ceram. Int.* 39, 2353 **(2013)**.

5. A. Famengo, S. Battiston, M. Saleemi, S. Boldrini, S. Fiameni, F. Agresti, M. S. Toprak, S. Barison, and M. Fabrizio, *J. Electron. Mater.* 42, 2020 **(2013)**.

6. E. Groβ, M. Riffel, and U. Stöhrer, *J. Mater. Res.* 10, 34 **(1995)**.

7. D. K. Shin, K. W. Jang, S. C. Ur, and I. H. Kim, *J. Electron. Mater.* 1 **(2013)**.

8. Y. Sadia, L. Dinnerman, and Y. Gelbstein, *J. Electron. Mater.* 42, 1926 **(2013)**.

9. W. Luo, H. Li, F. Fu, W. Hao, and X. Tang, *J. Electron. Mater.* 40, 1233 **(2011)**.

10. I. Aoyama, H. Kaibe, L. Rauscher, T. Kanda, M. Mukoujima, S. Sano, and T. Tsuji, *Japan J. Appl. Phys.* 44, 4275 **(2005)**.

11. G. Bernard-Granger, M. Soulier, H. Ihou-Mouko, C. Navone, M. Boidot, J. Leforestier, and J. Simon, *J. Alloys Compd.* 618, 403 **(2015)**.

12. D.-K. Shin, S.-W. You, and I.-H. Kim, *J. Korean Phys. Soc.* 64, 1412 **(2014)**.

13. S. Fiameni, S. Battiston, S. Boldrini, A. Famengo, F. Agresti, S. Barison, and M. Fabrizio, *J. Solid State Chem.* 193, 142 **(2012)**.

14. L. Lutterotti, S. Matthies, H. R. Wenk, A. S. Schultz, and J. W. Richardson, Jr., *J. Appl. Phys.* 81, 594 **(1997)**.

15. S. Boldrini, A. Famengo, F. Montagner, S. Battiston, S. Fiameni, M. Fabrizio, and S. Barison, *J. Electron. Mater.* 42, 1319 **(2013)**.

16. W. Luo, H. Li, Y. Yan, Z. Lin, X. Tang, Q. Zhang, and C. Uher, *Intermetallics* 19, 404 **(2011)**.

17. M. Saleemi, A. Famengo, S. Fiameni, S. Boldrini, S. Battiston, M. Johnsson, M. Muhammed, and M. S. Toprak, *J. Alloys Compd.* 619, 31 **(2015)**.

Received: 15 March 2016. Accepted: 14 June 2016.